Quantum phase transition in a three-level atom-molecule system

Sheng-Chang Li,[1,*] Li-Bin Fu,[2,3] and Fu-Li Li[1]
[1]*School of Science, Xi'an Jiaotong University, Xi'an 710049, China*
[2]*National Key Laboratory of Science and Technology on Computation Physics, Institute of Applied Physics and Computational Mathematics, Beijing 100088, China*
[3]*Center for Applied Physics and Technology, Peking University, Beijing 100084, China*
(Received 26 October 2012; published 1 July 2013)

We adopt a three-level bosonic model to investigate the quantum phase transition in an ultracold atom-molecule conversion system which includes one atomic mode and two molecular modes. Through thoroughly exploring the properties of energy-level structure, fidelity, and adiabatic geometric phase, we confirm that the system exhibits a second-order phase transition from an atom-molecule mixture phase to a pure molecule phase. We give the explicit expression of the critical point and obtain two scaling laws to characterize this transition. In particular, we find that both the critical exponents and the behavior of the ground-state geometric phase have obviously changed in contrast to a similar two-level model. Our analytical calculations show that the ground-state geometric phase jumps from zero to $\pi/3$ at the critical point. This discontinuous behavior has been checked by numerical simulations and it can be used to identify the phase transition in the system.

DOI: 10.1103/PhysRevA.88.013602 PACS number(s): 03.75.Hh, 05.30.Rt, 03.65.Vf, 67.85.Jk

I. INTRODUCTION

Quantum phase transition (QPT) is one of the most important concepts in the many-body quantum theory. As a central and fundamental transition phenomenon at the temperature of absolute zero, it describes an abrupt change in the ground state of a many-body system due to the quantum fluctuations [1,2]. The experimental observation of a QPT from a superfluid (SF) to a Mott insulator (MI) in a gas of ultracold atoms [3] inspired great interest in investigating clean, highly controllable, and strongly correlated bosonic systems [4]. Actually, the ultracold atomic gases [5] have become an ideal platform to study many-body physics because of their enormous applications and the advanced experimental techniques available in the fields of atomic and optical physics [6].

In recent years, a remarkable development in the aforementioned field is to convert ultracold atoms to molecules via Feshbach resonance [7–9] or photoassociation [10–12] techniques. Compared with the fermionic model in these kinds of systems, the bosonic model is of interest for theoretically exploring the QPTs. When both ultracold atoms and molecules are bosons, the systems possess a few degrees of freedom and a large particle number, which can greatly simplify the calculations. On the other hand, the atom-molecule conversion systems can be well described by the mean-field theory when the particle number is large enough. These features have stimulated a lot of effort to study the adiabatic evolution [13–18], geometric phase [19,20], and phase transition [21,22] of the systems. Instead of using the traditional approaches for describing a QTP (i.e., using the concepts of order parameter and symmetry breaking), recently Santos *et al.* adopted the concepts of entanglement and fidelity to investigate the QPT in a two-level bosonic atom-molecule system [21]. Motivated by this work, we discussed the same problem from the perspectives of scaling laws and Berry curvature [22]. However, the connection between the mean-field Berry phase and the phase transition in this type of bosonic model, and the properties of the QPT in a three-level atom-molecule system, remain unresolved, which calls for further theoretical considerations.

As a continuous work, in this paper we investigate the quantum phase transition in an ultracold atom-molecule conversion system by adopting a Λ-type three-level bosonic model. Based on this model, we first discuss the structure of quantum energy levels and analyze the properties of the ground state. In order to compare the phase-transition properties with a similar two-level model [21], we study the energy gap, the ground-state fidelity, and the mean-field geometric phase, respectively. We illustrate that when the ratio of the coupling strength between two molecular modes to the coupling strength between the atomic mode and the upper molecular mode exceeds a critical value, a similar QPT from a mixed atom-molecule phase to a pure molecular phase is also observed in our system. To characterize this transition, we derive the analytical expression of the critical point by using the mean-field approach and obtain two critical exponents via the study of scaling laws numerically. In particular, we find that this three-level system shows many striking properties that are different from the previous two-level model [19,21,22]: (i) The above two typical models belong to different universality classes due to the different scaling laws and critical exponents of QPTs. (ii) For the three-level model, the discontinuous behavior of the ground-state geometric phase at the critical point is similar to the topological index characterizing a topological phase transition. (iii) The behavior of the geometric phase is found to be a signal to identify the existence of the QPT in the system and suggests that one can further explore the underlying mechanism to classify QPTs according to the behavior of the geometric phase.

Our paper is organized as follow: In Sec. II, we give the second-quantized model and its mean-field description. In Sec. III, we explore the properties of energy levels and ground states. In Sec. IV, we choose the characteristic scaling law, fidelity, and adiabatic geometric phase to describe the QPT. Section V presents our conclusion.

*scli@mail.xjtu.edu.cn

II. THREE-LEVEL MODEL AND ITS MEAN-FIELD DESCRIPTION

The system we consider here is illustrated schematically in Fig. 1. It describes the process of creating ultracold diatomic molecules from bosonic condensed atoms, which constitutes a Λ-type three-level model. In the three-mode description, each mode $|\alpha\rangle$ ($\alpha = a, g$, and e represent the atomic mode, the ground-state molecular mode, and the excited-state molecular mode, respectively) is associated with an annihilation operator $\hat{\beta}$ ($\beta = a, b_g$, and b_e) due to the basic assumption that the spatial wave functions for these modes are fixed. By setting the energy of the atomic mode to zero, the Hamiltonian of the system takes the following second-quantized form with $\hbar = 1$ [20]:

$$\hat{H}_S = \omega_e \hat{b}_e^\dagger \hat{b}_e + \omega_g \hat{b}_g^\dagger \hat{b}_g + \left(\Omega_d e^{i\nu_d t} \hat{b}_e^\dagger \hat{b}_g + \frac{\Omega_p e^{-i\nu_p t}}{\sqrt{N}} \hat{b}_e^\dagger \hat{a}\hat{a} + \text{H.c.}\right), \quad (1)$$

where ν_d and ν_p are the frequencies of two laser pulses Ω_d and Ω_p, respectively. The frequencies ω_g and ω_e specify the molecular ground-state and excited-state energies, respectively. The total atom number $N = N_a + 2(N_g + N_e)$, with $N_a = \hat{a}^\dagger \hat{a}$, $N_g = \hat{b}_g^\dagger \hat{b}_g$, and $N_e = \hat{b}_e^\dagger \hat{b}_e$, commutes with the Hamiltonian (1) and is therefore conserved. Notice that the laser-pulse parameter Ω_p can be complex. To achieve this, one can split the laser pulse into two beams and then recombine and focus them on the system. As a result, we can express the complex parameter Ω_p as $\Omega_p = \xi_1 + \xi_2 e^{-i\varphi}$ with ξ_1 and ξ_2 being real numbers, where the phase factor φ is determined by the difference of optical paths between the two laser beams [20]. To carry out a comparative study to see the crucial differences between the three-level and two-level atom-molecule conversion systems, here we choose the above collisionless model and, in this case, the analytical solution can be obtained. The effects of particle interactions on the atom-molecule conversion efficiency and the QPT properties have been discussed in Refs. [23,24], respectively. The results showed that the particle interactions mainly change the critical point and slightly affect the critical exponents.

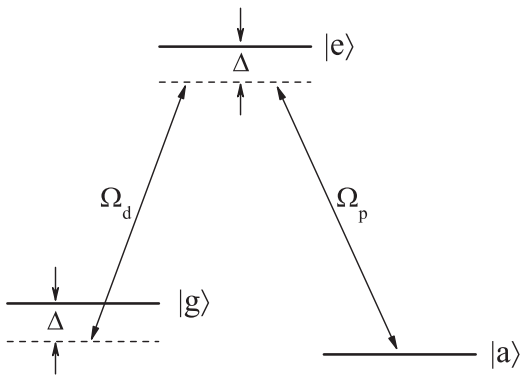

FIG. 1. Schematic diagram of a three-level atom-molecule conversion model coupled by two laser pulses Ω_d and Ω_p. The stable atomic state, the molecular ground state, and the molecular excited state are denoted by $|a\rangle$, $|g\rangle$, and $|e\rangle$, respectively. Δ measures the detuning of the pump laser Ω_p with respect to the transition from $|a\rangle$ to $|e\rangle$.

For convenience, we rewrite the above Schrödinger picture Hamiltonian as $\hat{H}_S = \hat{H}_0 + \hat{H}_1$, where

$$\hat{H}_0 = \nu_p \hat{b}_e^\dagger \hat{b}_e + (\nu_p - \nu_d)\hat{b}_g^\dagger \hat{b}_g, \quad (2)$$

$$\hat{H}_1 = (\omega_e - \nu_p)\hat{b}_e^\dagger \hat{b}_e + (\omega_g - \nu_p + \nu_d)\hat{b}_g^\dagger \hat{b}_g + \left(\Omega_d e^{i\nu_d t} \hat{b}_e^\dagger \hat{b}_g + \frac{\Omega_p e^{-i\nu_p t}}{\sqrt{N}} \hat{b}_e^\dagger \hat{a}\hat{a} + \text{H.c.}\right). \quad (3)$$

Then we choose $\omega_e = \omega_g + \nu_d$ and apply the interaction picture, i.e., $\hat{H}_I = e^{i\hat{H}_0 t} \hat{H}_1 e^{-i\hat{H}_0 t}$, and the Hamiltonian finally becomes

$$\hat{H}_I = \Delta(\hat{b}_e^\dagger \hat{b}_e + \hat{b}_g^\dagger \hat{b}_g) + \left(z\hat{b}_e^\dagger \hat{b}_g + \frac{\rho e^{-i\phi}}{\sqrt{N}} \hat{b}_e^\dagger \hat{a}\hat{a} + \text{H.c.}\right), \quad (4)$$

where the parameters $\Delta = \omega_e - \nu_p$, $z = \Omega_d$, $\rho = |\Omega_p|$, and $\phi = \arg(\Omega_p)$ have been introduced.

To complement the quantum description and gain insight into the existence of a QPT in our model, we adopt a semiclassical description of the system following the usual mean-field approach, which has been proven to be a powerful tool for studying ultracold atoms and Bose-Einstein condensates (BECs). In the semiclassical limit $N \to \infty$, the quantum model becomes classical and one can replace the operator $\hat{\beta}$ with a corresponding complex number β ($\beta = a, b_g, b_e$), i.e., $\mathcal{H} = \Delta(|b_e|^2 + |b_g|^2) + z(b_e^* b_g + b_g^* b_e) + \rho[e^{-i\phi} b_e^* a^2 + e^{i\phi} b_e (a^*)^2]$. Using the equations $i d\beta/dt = \partial\mathcal{H}/\partial\beta^*$, we can obtain the following Schrödinger equations with the normalization condition $|a|^2 + 2(|b_g|^2 + |b_e|^2) = 1$ to govern the dynamical behavior of the system:

$$i\frac{d}{dt}|\psi\rangle = H_{mf}|\psi\rangle, \quad (5)$$

where

$$H_{mf} = \begin{pmatrix} 0 & 0 & 2\rho e^{i\phi} a^* \\ 0 & \Delta & z \\ \rho e^{-i\phi} a & z & \Delta \end{pmatrix}, \quad (6)$$

and $|\psi\rangle = (a, b_g, b_e)^T$. In this system, the mean-field Hamiltonian $\mathcal{H}$ contains terms $b_e^* a^2$ and $b_e (a^*)^2$ describing the coupling between atom pairs and diatomic molecules, which obviously does not have U(1) gauge invariance. We notice that even though the Hamiltonian matrix H_{mf} is not conjugate symmetric, the original system represented by Eq. (4) is Hermitian and the total system energy is bound. When the particles are bosons and the number of particles in the system is large, the quantum system can be well described by the mean-field Hamiltonian. In this description, the system can be cast into a nonlinear system due to the fact that creating one molecule needs two atoms. Mathematically, the mean-field Hamiltonian H_{mf} is a function of the instantaneous wave function as well as its conjugate. It is a non-Hermitian matrix and invariant under the following transformation [18]:

$$|\psi\rangle \to U_s|\psi\rangle = e^{i\Theta(\theta)}|\psi\rangle = e^{i\begin{pmatrix} \theta & 0 & 0 \\ 0 & 2\theta & 0 \\ 0 & 0 & 2\theta \end{pmatrix}}|\psi\rangle. \quad (7)$$

The lack of U(1) gauge transformation is a particularly interesting point of the above mean-field model, which may lead to some new properties of the system. In the subsequent sections, based on models (4) and (5), we will discuss the QPT in the system from both the fully quantum and the mean-field perspectives.

III. ENERGY LEVELS AND GROUND STATES

Since N is conserved, one can diagonalize the quantum Hamiltonian $\hat{H}_I$. For simplicity, hereafter we assume that N is even; then the Hilbert space of the N-particle system can be reduced to $\frac{1}{2}(\frac{N}{2}+1)(\frac{N}{2}+2)$ dimension in the Fock basis, i.e., $|n_a\rangle|n_g\rangle|n_e\rangle = (n_a!n_g!n_e!)^{-1/2}(\hat{a}^\dagger)^{n_a}(\hat{b}_g^\dagger)^{n_g}(\hat{b}_e^\dagger)^{n_e}|0\rangle$ with $|0\rangle$ being the vacuum state, where $n_g = 0,1,\ldots,\frac{N}{2}$, $n_e = 0,1,\ldots,\frac{N}{2}-n_g$, and $n_a = N-2(n_g+n_e)$ represent the particles in states $|b_g\rangle$, $|b_e\rangle$, and $|a\rangle$, respectively. By directly diagonalizing the Hamiltonian matrix with a fixed N, we obtain the eigenenergy levels and the ground states of the system as shown in Figs. 2 and 3, respectively.

It is well known that a typical Λ-type three-level system supports dark-state solutions with zero eigenvalue [16,25,26]. This type of state can result in a phenomenon known as coherent population trapping (CPT). For our system, when $\Delta = 0$, from Figs. 2(b)–2(d) we see that the energy levels with energy value being zero are degenerate, while other nonzero-energy levels are nondegenerate and are symmetrically distributed in both sides of the center level. This symmetric energy structure is determined by the symmetry of the Hamiltonian

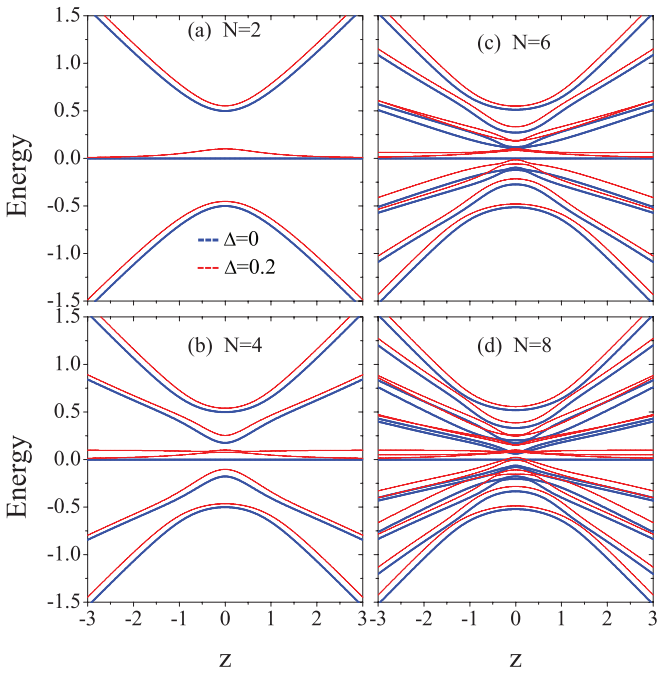

FIG. 2. (Color online) Quantum energy levels for different particle numbers: (a) $N = 2$, (b) $N = 4$, (c) $N = 6$, and (d) $N = 8$. The thick and thin lines denote the cases $\Delta = 0$ and $\Delta = 0.2$, respectively. The energies are shown in units of $N\rho$, while the parameters z and Δ are rescaled by ρ.

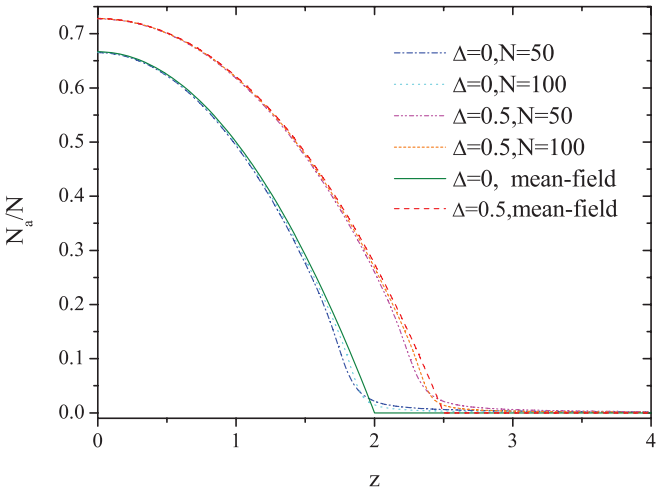

FIG. 3. (Color online) Atomic fraction in the ground state vs the parameter z with $\Delta = 0$ and $\Delta = 0.5$. Both z and Δ are rescaled by ρ.

$\hat{H}_I$ with $\phi = 0$, i.e., the change of variables $(z,\rho) \to -(z,\rho)$ is equivalent to the unitary transformation $\hat{b}_e \to -\hat{b}_e$. In this case, the degeneracy of the zero-energy level (i.e., d) is given by

$$d = \left\lceil \left(\frac{N}{2}+1\right) \Big/ 2 \right\rceil = \frac{1}{4}(N - \mathrm{Mod}[N,4]) + 1. \quad (8)$$

The symbol $\lceil\ \rceil$ stands for the ceiling function, which maps a real number to the smallest following integer.

Notice that if the parameter Δ has a perturbation, the symmetry mentioned above of the system with $\Delta = 0$ will be broken. This leads to the shift of the energy levels and the zero-energy level splitting. For example, when $\Delta = 0.2$ and $N = 8$ [see Fig. 1(d)], all energy levels are pushed up and the zero-energy level is split into three nonzero-energy levels. For different N, the maximum number of energy levels should be $(\frac{N}{2}+1)(\frac{N}{2}+2)/2$.

Now we discuss the ground-state properties which are closely associated with the QPT in the system. On one hand, by diagonalizing the Hamiltonian $\hat{H}_I$ numerically, for both $\Delta = 0$ and $\Delta \neq 0$, we calculated the ground states with different total atom numbers. The results for the atomic population fraction (i.e., N_a/N) in the ground state are demonstrated in Fig. 3. We found that the atomic fraction in the ground state decreases and gradually approaches zero as the ratio of the coupling strength between two molecule modes to that between the atom mode and the molecular mode increases. On the other hand, we study the ground state from the mean-field perspective. Based on model (5), we obtain the mean-field ground state from the eigenequation $H_{\mathrm{mf}}(\bar{a}^*,\bar{a})|\bar{\psi}\rangle = \Theta(\mu)|\bar{\psi}\rangle$ with μ being the chemical potential for atoms and $|\bar{\psi}\rangle$ being the eigenstate. For $\Delta = 0$, $z \geqslant 0$, and $\rho > 0$, we obtain the eigenvalue, and the corresponding eigenfunction for the ground state is as follows:

$$\mu_0 = \begin{cases} -\frac{z}{2}, & z > 2\rho, \\ -\frac{(z^2-2\rho^2)\sqrt{z^2+8\rho^2}}{4\sqrt{3}\rho^2}, & z < 2\rho; \end{cases} \quad (9)$$

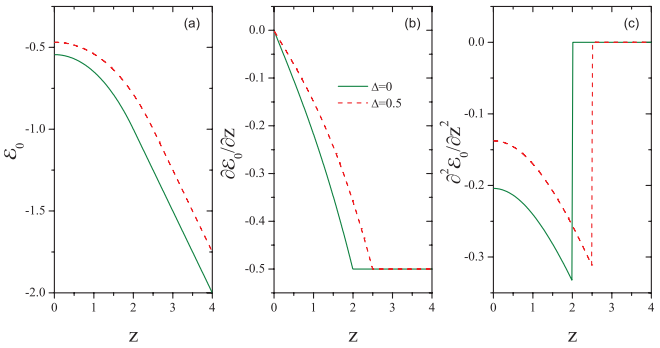

FIG. 4. (Color online) (a) The energy of the mean-field ground state and its (b) first and (c) second derivatives with respect to coupling parameter z. The parameters z and Δ are rescaled by ρ.

$$|\bar{\psi}_0\rangle = \begin{cases} \begin{pmatrix} 0 \\ \frac{1}{2} \\ -\frac{1}{2} \end{pmatrix}, & z > 2\rho, \\ \begin{pmatrix} \frac{\sqrt{4-z^2/\rho^2}}{\sqrt{6}} \\ \frac{z}{4\rho}e^{-i\phi} \\ -\frac{\sqrt{z^2+8\rho^2}}{4\sqrt{3}\rho}e^{-i\phi} \end{pmatrix}, & z < 2\rho. \end{cases} \tag{10}$$

For $\Delta \neq 0$, although the solutions to the ground state can also be obtained analytically, the expressions are generally too messy to be instructive. We therefore simply display the results in Fig. 3. From Fig. 3, we found that for both $\Delta = 0$ and $\Delta \neq 0$, the results for the quantum model (4) approach the analytical mean-field results with increasing the total particle number N.

It should be mentioned that for the nonlinear system (5), the classical energy $\mathcal{E}$ is not equal to the chemical potential, and the relation between them is $\mathcal{E} = \mu \pm \rho|\bar{b}_e||\bar{a}|^2$. We have calculated the ground-state energy $\mathcal{E}_0$ analytically and find its second derivative possesses a discontinuity at a critical point $z_c = 2\rho + \Delta$, as shown in Fig. 4. This divergence behavior implies that the system will undergo a second-order phase transition in the thermodynamic limit. When $z < z_c$, the system is in an atom-molecule mixture phase (i.e., $|\bar{a}|^2 > 0$), and when $z > z_c$, the system is in a pure molecule phase where $|\bar{a}|^2 = 0$. In the mixture phase, the asymptotic behavior of the ground state in the vicinity of the critical point with $\Delta = 0$ is given by the variation of the parameter $s_0 = |\bar{a}|^2$, i.e.,

$$s_0|_{z\to z_c} = \tfrac{1}{6}[4 - z_c(2z - z_c)]. \tag{11}$$

IV. QUANTUM PHASE TRANSITION

In the previous section, we demonstrated that the process of converting ultracold atoms to homonuclear diatomic molecules in a bosonic system is a QPT, which differs from the well-known BCS-BEC crossover phenomena in fermionic systems [27,28]. Now, we will describe and characterize this phase transition from different perspectives.

A. Scaling laws

In order to understand the QPT in the system, we begin our discussion by analyzing the dimensionless energy gap between the first excited state and the ground state, namely, $\Delta E = (E_1 - E_0)/\rho$. With the help of diagonalizing the Hamiltonian (4) numerically, we calculated the energy levels with different particle numbers. For a fixed N, the energy gap takes a minimum value at a point z_N (it can be viewed as a pseudocritical point of the N-particle system) and this point just corresponds to the position of avoided level crossing (see Fig. 2). Generally, the QPTs often occur at positions of level crossings or avoided level crossings. As our system undergoes avoided level crossings, the existence of the minimum of the energy gap indicates a basic signature of the phase transition. Similar to the phenomena studied in a two-level atom-molecule system [21] and in other systems, we found that the gap ΔE in our system also approaches zero at a single point rather than over an interval of the dimensionless parameter z/ρ with the particle number $N \to \infty$. This specific phenomenon implies that when $N \to \infty$, the ground state is degenerate at the point z_c where there is no phase, which is a requirement for the occurrence of a broken-symmetry phase [21].

To capture more features of QPT in the system, we study the scaling behavior of the energy gap near the critical point. To this end, we first calculate the energy gap for different values of parameter Δ and the results are shown in Fig. 5. Either for the variation of the total atomic number N versus $|z_N - z_c|$ [see Fig. 5(a)] or for the change of the minimum of the energy gap (i.e., $\Delta E_{\min}$) with respect to N [see Fig. 5(b)], the same characteristic scaling laws have been observed for different Δ, and different curves in each figure with a same slope give the evidence.

In the quantum model (4), the total atom number N can be regarded as a correlation length scale of the system, and then one can connect this length scale to the offset between the pseudocritical point and the critical point. Quantificationally, we have

$$\kappa|z_c - z_N|^{\nu} \simeq N^{-1}, \tag{12}$$

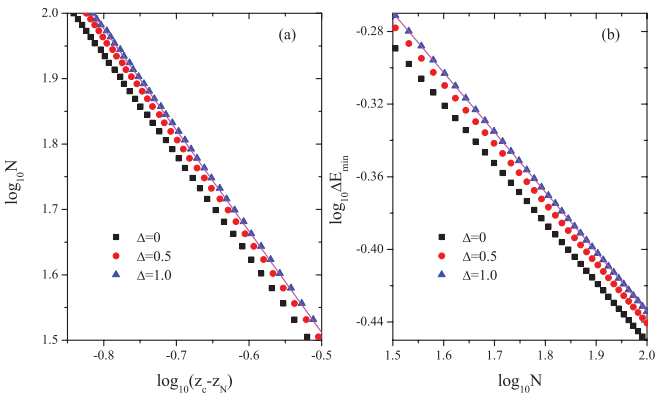

FIG. 5. (Color online) (a) The total atomic number N vs the offset between z_N and z_c. (b) The minimum value of the energy gap (i.e., $\Delta E_{\min}$) at the pseudocritical point z_N vs N. Solid lines are plotted for guiding eyes, respectively, with the slopes being -1.54764 and -0.32912 (from left to right).

where $\nu \simeq 1.54764$ is a critical exponent and $\kappa \simeq 0.18273$ is an inessential constant. This scaling law shows that the pseudocritical point changes and approaches the critical point as $N^{-1/\nu}$ and clearly approaches z_c as $N \to \infty$ [see Fig. 5(a)]. From Fig. 5(b), we find another scaling law, that is

$$\Delta E_{\min}/N \simeq \Gamma N^{-\zeta}, \tag{13}$$

where $\Gamma \simeq 1.67506$ is a constant. $\zeta \simeq 1.32912$ gives another important exponent, namely, the dynamic critical exponent. We should mention that all constants and exponents given in the above two formulas are obtained in the case of $\Delta = 0$. For other cases, their values may change slightly. Comparing the product of two exponents in our system with that of a two-level atom-molecule system [22], we find that the values are obviously different. This difference indicates that the above two models belong to different universality classes.

B. Fidelity

Similar to other concepts, the behavior of the fidelity can also be employed to identify the phase transition [29,30]. The fidelity is a measure of the distance between two states and this concept has been widely used in the field of quantum information [31]. One can define fidelity through the modulus of the wave-function overlap between two states, i.e.,

$$F(\psi_1, \psi_2) = |\langle \psi_1 | \psi_2 \rangle|. \tag{14}$$

Here we only focus on the behavior of the fidelity between two ground states. One ground state is obtained when $\Delta = 0$, namely, $|\Delta = 0\rangle$, and the other ground state is calculated by treating Δ as a perturbation parameter, denoted as $|\Delta \neq 0\rangle$. We have estimated the wave-function overlap between two ground states with different particle number N while varying parameter Δ. Figure 6 shows the fidelity between the ground state $|\Delta = 0\rangle$ and the ground state $|\Delta = \alpha\rangle$ with $\alpha = 0.1, 0.2, 0.3$, and 0.4. For both $N = 50$ and $N = 100$, we can see that the fidelity $|\langle \Delta = 0 | \Delta \neq 0 \rangle|$ shows dip behavior at the point corresponding to the pseudocritical point. The results imply that the two ground states are distinguishable and there is an obvious signal for the QPT as long as $\alpha \neq 0$. Moreover, we observe that the dip of the ground-state fidelity becomes deeper and the point where the fidelity has a minimum varies with increasing of the value of α; this phenomenon is very different from that in a two-level atom-molecule model where the fidelity has a minimum at the same point [21]. The reason is that in our model, the phase-transition point z_c is determined by the relation $z_c = 2\rho + \Delta$. For a larger α, we found that the distinguishability of the two states increases and the position of the minimum of the fidelity evidently changes.

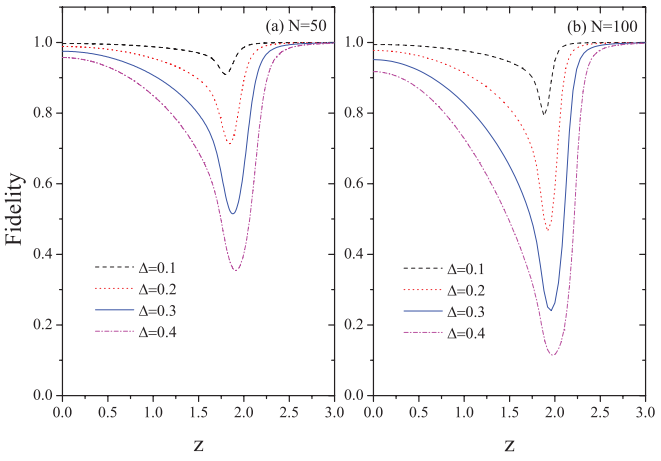

FIG. 6. (Color online) Ground-state fidelity vs the parameter z with (a) $N = 50$ and (b) $N = 100$ for different Δ. The parameters Δ and ρ are rescaled by ρ.

We compare the results obtained in the case of $N = 50$ with the results for $N = 100$. For the same Δ, it is seen that the position of the minimum fidelity for $N = 100$ is closer to the critical point z_c than that for $N = 50$. In fact, we have calculated the ground-state fidelity with varying the particle number N and find that for a fixed α, with increasing N, the overlap between the two states becomes smaller (i.e., the two states are more distinguishable) and the position where the minimum fidelity occurs moves toward $2\rho + \Delta$. Thus, in the finite particle number case, the occurrence of the minima of the fidelity gives information about the phase transition in the system.

C. Geometric phase

In this section, we investigate the behavior of the ground-state geometric phase starting from the mean-field model (5). In the following, to obtain analytical results, we focus our attention on the case where the detuning is absent (i.e., $\Delta = 0$). To employ the procedures for calculating geometric phase in nonlinear systems proposed in Refs. [19,32], we introduce some variables, namely, $a = \sqrt{1 - 2(p_1 + p_2)}e^{i\lambda}$, $b_g = \sqrt{p_1}e^{i(2\lambda + q_1)}$, and $b_e = \sqrt{p_2}e^{i(2\lambda + q_2)}$, where $\lambda = \arg(a)$ denotes the total phase, $p_1 = |b_g|^2$ and $p_2 = |b_e|^2$ are the population probabilities of the ground-state and the excited-state molecules, respectively, and $q_1 = \arg(b_g) - 2\arg(a)$ and $q_2 = \arg(b_e) - 2\arg(a)$ are the relative phases. With the help of these variables, the three-level system can be cast into a classical Hamiltonian,

$$\begin{aligned}\mathcal{H} = {} & 2z\sqrt{p_1 p_2}\cos(q_1 - q_2) \\ & + 2\rho\sqrt{p_2}[1 - 2(p_1 + p_2)]\cos(q_2 + \phi).\end{aligned} \tag{15}$$

The Schrödinger equations (5) together with the normalization condition lead to

$$\frac{d\lambda}{dt} = -2\rho\sqrt{p_2}\cos(q_2 + \phi), \tag{16}$$

and

$$\frac{dp_i}{dt} = -\frac{\partial \mathcal{H}}{\partial q_i}, \frac{dq_i}{dt} = \frac{\partial \mathcal{H}}{\partial p_i}, \tag{17}$$

with $i = 1$ and 2. These four equations have established a connection between the projected Hilbert space spanned by $\mathbf{S}(p_i, q_i)$ and the parameter space spanned by $\mathbf{R}(z, \rho, \phi)$.

To calculate the geometric phase for the ground state of the system, for simplicity, we construct a closed loop C in the parameter space by treating z and ρ as constants and varying ϕ from 0 to 2π with time. The system is assumed to evolve adiabatically along the cyclic path with rate $\epsilon = |\frac{d\phi}{dt}| \sim \frac{1}{T}$, where T is the period of the cyclic evolution. Initially, we prepare the system in the ground state of $H_{mf}(\phi = 0)$, and after a cyclic adiabatic evolution, the state acquires

a geometric phase besides the dynamical phase. Since the adiabatic parameter $\epsilon \ll 1$, it can be regarded as a small parameter during the process for determining the geometric phase. Following the method in Ref. [32], we expand $d\lambda/dt$ in a perturbation series in ϵ, i.e.,

$$\frac{d\lambda}{dt} = \lambda_0(\epsilon^0) + \lambda_1(\epsilon^1) + O(\epsilon^2), \tag{18}$$

to separate the pure geometric part from the total phase. The time integrals of the zero-order term and the first-order term in Eq. (18) give the dynamic phase and the geometric phase in the adiabatic limit, $\epsilon \to 0$ or $T \to \infty$, respectively, and the contribution from the higher-order terms will vanish.

During the adiabatic evolution, the system fluctuates around the ground state due to the small but finite value of ϵ. This fact allows us to expand the variables as $p_i = \bar{p}_i(\mathbf{R}) + \delta p_i(\mathbf{R})$ and $q_i = \bar{q}_i(\mathbf{R}) + \delta q_i(\mathbf{R})$ with $i = 1$ and 2, where $(\bar{p}_i, \bar{q}_i)$ stand for the instantaneous ground state, and δp_i and δq_i denote the fluctuations induced by the slow change of the system. By substituting these expressions back into Eq. (16), when $z < 2\rho$, we have

$$\lambda_0 = -\mu_0(\mathbf{R}), \tag{19}$$

$$\lambda_1 = \frac{-2\bar{p}_2\sqrt{\bar{p}_1}z + \rho[\bar{p}_2(6\bar{p}_2 + 6\bar{p}_1 - 1) + \delta p_2]}{\sqrt{\bar{p}_2}}, \tag{20}$$

where the chemical potential of the ground state is $\mu_0 = -2z\sqrt{\bar{p}_1\bar{p}_2} - 3\rho\sqrt{\bar{p}_2}[1 - 2(\bar{p}_1 + \bar{p}_2)]$. Moreover, from Eqs. (17), we have

$$\delta p_2 = \frac{2\sqrt{\bar{p}_2}\left(z\bar{p}_2 + z\bar{p}_1 - 4\rho\bar{p}_1^{3/2}\right)}{\rho\left[z(1 + 6\bar{p}_2 + 6\bar{p}_1) - 16\rho\bar{p}_1^{3/2}\right]}\frac{d\phi}{dt}. \tag{21}$$

To deduce Eqs. (20) and (21), we have used the fixed-point equations $\frac{\partial\mathcal{H}}{\partial p_i}|_{(\bar{p}_i,\bar{q}_i)} = 0$ and the condition $\frac{d}{dt}\delta q_i \sim O(\epsilon^2)$. Combining Eq. (21) with Eq. (20), and using the fixed-point values corresponding to the ground state, i.e., $(\bar{p}_1, \bar{q}_1; \bar{p}_2, \bar{q}_2) = (\frac{z^2}{16\rho^2}, \bar{q}_2 \pm \pi; \frac{z^2+8\rho^2}{48\rho^2}, \pm\pi - \phi)$, we obtain

$$\lambda_1 = \frac{1}{6}\frac{d\phi}{dt}. \tag{22}$$

Integrating Eq. (22) over T with respect to time, we have

$$\lambda_g = \int_0^T \lambda_1 dt = \frac{1}{6}\int_0^{2\pi} d\phi = \frac{\pi}{3}. \tag{23}$$

For comparison, we give the result that is directly calculated from the Berry's formula [33], i.e.,

$$\lambda_b = i\int_0^{2\pi} \langle\bar{\psi}_0|\nabla_\phi|\bar{\psi}_0\rangle d\phi = \frac{\pi}{6}\left(2 + \frac{z^2}{\rho^2}\right). \tag{24}$$

Now we consider the situation $z > 2\rho$. In this case, the ground state, i.e., $\bar{p}_1 = \bar{p}_2 = 1/4$, is independent of the parameter $\mathbf{R}$. Simple calculations from Eqs. (16) and (17) lead to

$$\frac{d\lambda}{dt} = \frac{z}{2} = -\mu_0, \tag{25}$$

and then

$$\lambda = \int_0^T \lambda_0 dt = -\int_0^T \mu_0 dt = \lambda_d. \tag{26}$$

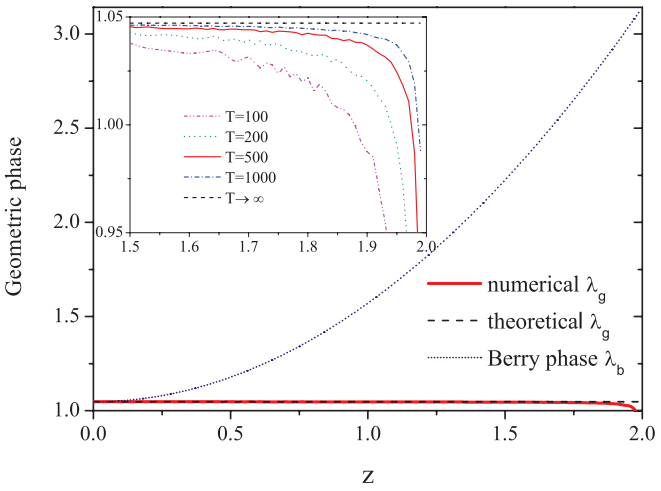

FIG. 7. (Color online) Comparison between the numerical results for the ground-state geometric phase with $T = 500$ and the analytical results given by Eq. (23). The dotted line denotes the results obtained from Berry's formula. The inset illustrates the numerical results around the critical point with different T. The parameter z is rescaled by ρ.

This result implies that the geometric phase $\lambda_g = 0$ in the case $z > 2\rho$. In summary, the above theoretical calculations demonstrate that the mean-field geometric phase of the ground state jumps from zero to $\pi/3$ when the system undergoes the phase transition from a mixture phase to a pure molecular phase. These analytical predictions have been checked by numerically solving Eq. (5) or Eqs. (16) and (17), as illustrated in Fig. 7. We see that if the evolution period T is large enough, the simulated results show a good agreement with the analytical prediction. We use Fig. 8 to exhibit the convergence behaviors of the ground-state and the geometric phase with increasing T, and a large convergence rate has been observed. It is worth emphasizing that different values of the geometric phase in different parameter regions can be an evident signature of the QPT in the system.

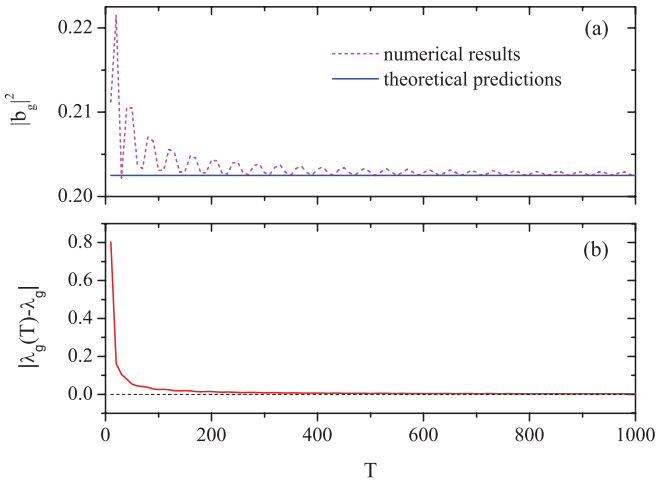

FIG. 8. (Color online) The convergence of population in the (a) ground-state molecular mode and (b) geometric phase, with respect to the evolution period T for $z/\rho = 1$.

V. CONCLUSION

We have investigated the quantum phase transition in a three-level atom-molecule conversion system. By using different approaches, we confirm that the system exhibits a second-order phase transition which is similar to a QPT exhibited in a two-level bosonic model [21]. First, through analyzing the properties of the energy gap, we derive two scaling laws and the corresponding critical exponents. It was found that the two-level model and our model belong to different universality classes. Second, we discuss the ground-state fidelity. A minimum value of the fidelity near the critical point has been found. Finally, we have calculated the ground-state geometric phase, and a discontinuous behavior at the critical point has been shown. This phenomenon is similar to that studied in a system of a Bose-Einstein condensate in an optical cavity [34]. It establishes a connection between the ground-state geometric phase and the QPT in an interacting atom-molecule bosonic model following the early works in a spin-chain system [35,36]. In summary, we have studied the characteristic scaling laws of the QPT and given the connection between the abrupt change behavior of the ground-state geometric phase at the critical point and the QPT. Our mean-field geometric phase might potentially be observable in future experiments due to the significant development in the field of creating ultracold molecules via Feshbach resonances [37] or a stimulated Raman transition [10,38]. Our findings also suggest that one can further explore the underlying mechanism to classify QPTs according to the behavior of the geometric phase.

ACKNOWLEDGMENTS

This work is supported by the National Fundamental Research Program of China (Contract No. 2011CB921503), the National Natural Science Foundation of China (Contracts No. 10725521, No. 91021021, No. 11075020, No. 11005055, and No. 11078001), and the Fundamental Research Funds for the Central Universities of China.

[1] S. Sachdev, *Quantum Phase Transitions* (Cambridge University Press, Cambridge, UK, 1999); M. Vojta, Rep. Prog. Phys. **66**, 2069 (2003).
[2] S. L. Sondhi, S. M. Girvin, J. P. Carini, and D. Shahar, Rev. Mod. Phys. **69**, 315 (1997).
[3] M. Greiner, O. Mandel, T. Esslinger, T. W. Hänsch, and I. Bloch, Nature (London) **415**, 39 (2002).
[4] D. Tilahun, R. A. Duine, and A. H. MacDonald, Phys. Rev. A **84**, 033622 (2011).
[5] See, e.g., L. Pitaevskii and S. Stringari, *Bose-Einstein Condensation* (Clarendon, Oxford, 2003).
[6] J. Ruseckas, G. Juzeliūnas, P. Öhberg, and M. Fleischhauer, Phys. Rev. Lett. **95**, 010404 (2005).
[7] E. A. Donley, N. R. Claussen, S. T. Thompson, and C. E. Wieman, Nature (London) **417**, 529 (2002).
[8] K. Xu, T. Mukaiyama, J. R. Abo-Shaeer, J. K. Chin, D. E. Miller, and W. Ketterle, Phys. Rev. Lett. **91**, 210402 (2003).
[9] J. Herbig, T. Kraemer, M. Mark, T. Weber, C. Chin, H.-C. Nägerl, and R. Grimm, Science **301**, 1510 (2003).
[10] R. Wynar, R. S. Freeland, D. J. Han, C. Ryu, and D. J. Heinzen, Science **287**, 1016 (2000).
[11] T. Rom, T. Best, O. Mandel, A. Widera, M. Greiner, T. W. Hänsch, and I. Bloch, Phys. Rev. Lett. **93**, 073002 (2004).
[12] K. Winkler, G. Thalhammer, M. Theis, H. Ritsch, R. Grimm, and J. H. Denschlag, Phys. Rev. Lett. **95**, 063202 (2005).
[13] U. Gaubatz, P. Rudecki, M. Becker, S. Schiemann, M. Külz, and K. Bergmann, Chem. Phys. Lett. **149**, 463 (1988).
[14] J. R. Kuklinski, U. Gaubatz, F. T. Hioe, and K. Bergmann, Phys. Rev. A **40**, 6741 (1989).
[15] E. Pazy, I. Tikhonenkov, Y. B. Band, M. Fleischhauer, and A. Vardi, Phys. Rev. Lett. **95**, 170403 (2005).
[16] H. Y. Ling, P. Maenner, W. Zhang, and H. Pu, Phys. Rev. A **75**, 033615 (2007).
[17] E. A. Shapiro, M. Shapiro, A. Peer, and J. Ye, Phys. Rev. A **75**, 013405 (2007).
[18] S.-Y. Meng, L.-B. Fu, and J. Liu, Phys. Rev. A **78**, 053410 (2008).
[19] L. B. Fu and J. Liu, Ann. Phys. **325**, 2425 (2010).
[20] F. Cui and B. Wu, Phys. Rev. A **84**, 024101 (2011).
[21] G. Santos, A. Foerster, J. Links, E. Mattei, and S. R. Dahmen, Phys. Rev. A **81**, 063621 (2010).
[22] S. C. Li and L. B. Fu, Phys. Rev. A **84**, 023605 (2011).
[23] J. Li, D. F. Ye, C. Ma, L. B. Fu, and J. Liu, Phys. Rev. A **79**, 025602 (2009).
[24] N.-J. Hui, L.-H. Lu, X.-Q. Xu, and Y.-Q. Li, arXiv:1212.6884.
[25] H. Pu, P. Maenner, W. Zhang, and H. Y. Ling, Phys. Rev. Lett. **98**, 050406 (2007).
[26] H. Y. Ling, H. Pu, and B. Seaman, Phys. Rev. Lett. **93**, 250403 (2004).
[27] C. A. Regal, M. Greiner, and D. S. Jin, Phys. Rev. Lett. **92**, 040403 (2004); G. B. Partridge, K. E. Strecker, R. I. Kamar, M. W. Jack, and R. G. Hulet, *ibid.* **95**, 020404 (2005).
[28] J. Links, H. Q. Zhou, R. H. McKenzie, and M. D. Gould, J. Phys. A **36**, R63 (2003); G. Santos, A. Tonel, A. Foerster, and J. Links, Phys. Rev. A **73**, 023609 (2006).
[29] P. Zanardi and N. Paunković, Phys. Rev. E **74**, 031123 (2006).
[30] H.-Q. Zhou and J. P. Barjaktarevic, J. Phys. A **41**, 412001 (2008).
[31] M. A. Nielsen and I. L. Chuang, *Quantum Computation and Quantum Information* (Cambridge University Press, Cambridge, UK, 2000).
[32] J. Liu and L. B. Fu, Phys. Rev. A **81**, 052112 (2010).
[33] M. V. Berry, Proc. R. Soc. London, Ser. A **392**, 45 (1984).
[34] S. C. Li, L. B. Fu, and J. Liu, Phys. Rev. A **84**, 053610 (2011).
[35] A. C. M. Carollo and J. K. Pachos, Phys. Rev. Lett. **95**, 157203 (2005).
[36] S.-L. Zhu, Phys. Rev. Lett. **96**, 077206 (2006).
[37] D. Kleppner, Phys. Today **57**, 12 (2004).
[38] B. LaburtheTolra, C. Drag, and P. Pillet, Phys. Rev. A **64**, 061401 (2001).